

Traps for Electrons and Holes Limit the Efficiency and Durability of Polymer Light-Emitting Electrochemical Cells

Matthias Diethelm, Andrius Devižis, Wei-Hsu Hu, Tao Zhang, Roman Furrer, Camilla Vael, Sandra Jenatsch, Frank Nüesch, and Roland Hany*

Polymer light-emitting electrochemical cells (PLECs) and light-emitting diodes (PLEDs) receive interest for large-area lighting and signage applications. During operation of a PLEC, a p–i–n junction develops where electrons and holes are injected into the film and are transported along *n*- and *p*-doped regions to the intrinsic (*i*) region, where they recombine under light emission. Conceptually, this resembles the PLED device architecture equipped with Ohmic charge-injection and transport layers. The similarity between the *i*-region of the PLEC and the emissive layer of the PLED is obvious; however, implication of this has not been examined in detail so far. For example, for PLEDs it is known that electron traps hinder the electron transport, and that hole trap formation dictates the long-term durability. Here, for PLECs the electrical and optical response to electrical driving and breaks are studied, the current response to external light irradiation is probed, and degradation is followed with long-term absorption and capacitance measurements. The electron traps in PLECs are identified and it is found that hole trap formation limits the device lifetime, in the same manner as established for PLEDs. It is concluded that charge traps in semiconducting polymers present important, but so far overlooked intrinsic performance limitations for PLECs.

1. Introduction

Polymer light-emitting electrochemical cells (PLECs) are one of the simplest electroluminescent devices and consist of a single solution-processed emissive polymer layer that contains an electrolyte, sandwiched between two air-stable electrodes.^[1–9] When a bias is applied, the ions redistribute and the homogeneous polymer film divides into five sublayers with specific functions.^[10] First, the ions form electric double layers (EDLs) at both electrodes that facilitates charge injection. Subsequently, reduced and oxidized polymer repeating units (*n*- and *p*-polarons) are electrostatically stabilized by opposite ionic charges, resulting in conductive *p*- and *n*-doped regions at the anode and cathode, respectively, which grow inside the film. Over time, a p–i–n junction develops where holes and elec-

trons are injected from the electrodes into the film and travel along the doped regions to the intrinsic (*i*) zone, where they recombine under the emission of light. The PLEC turn-on dynamics is dictated by the mobility of the ions,^[10,11] and the time scale until ions are in equilibrium ranges from seconds to many hours.^[4,11,12] A second timescale to consider is the relaxation time of the ions back to equilibrium when an operated PLEC in steady state is turned off. This time usually is even longer than the turn-on time and can reach up to several days.^[11]

The “EDL–p–i–n–EDL” buildup in an operated PLEC strongly resembles the multilayer architecture of an organic light-emitting diode (OLED). For example, the functionality of charge-injection and -transport layers in the OLED are identified with the role the EDLs and doped regions play in the PLEC. Therefore, despite the different device architecture and dynamic turn-on behavior, the mode of operation of PLEDs and PLECs—after steady state is reached—is quite comparable (Figure S1, Supporting Information).

We focus on the similarity between the emissive layers of a PLED and a PLEC, as the PLEC *i*-region is also void of ions and the place where excitons form and light emission occurs. We argue that a physical characteristic pertinent to the emissive polymer in a PLED can also be detected in a PLEC. Specifically, it is known that the efficiency and lifetime of PLEDs is seriously limited by the presence of traps for electrons and holes.^[13] Trapped charges hinder the charge transport and increase

M. Diethelm, W.-H. Hu, T. Zhang, F. Nüesch, R. Hany
Empa
Swiss Federal Laboratories for Materials Science and Technology
Laboratory for Functional Polymers
Dübendorf 8600, Switzerland
E-mail: roland.hany@empa.ch


M. Diethelm, W.-H. Hu, T. Zhang, C. Vael, F. Nüesch
EPFL

Institute of Materials Science and Engineering
Ecole Polytechnique Fédérale de Lausanne
Station 12, Lausanne 1015, Switzerland

A. Devižis
State Research Institute Center for Physical Sciences and Technology
Saulėtekio av. 3, Vilnius LT-10257, Lithuania

R. Furrer
Empa
Swiss Federal Laboratories for Materials Science and Technology
Transport at Nanoscale Interfaces
Dübendorf 8600, Switzerland

C. Vael, S. Jenatsch
Fluxim AG
Katharina-Sulzer-Platz 2, Winterthur 8400, Switzerland

 The ORCID identification number(s) for the author(s) of this article can be found under <https://doi.org/10.1002/adfm.202203643>.

© 2022 The Authors. Advanced Functional Materials published by Wiley-VCH GmbH. This is an open access article under the terms of the Creative Commons Attribution License, which permits use, distribution and reproduction in any medium, provided the original work is properly cited.

DOI: 10.1002/adfm.202203643

the nonradiative Shockley–Read–Hall (SRH) recombination between trapped and free charge, thereby reducing the radiative Langevin recombination and the device efficiency. It has been shown that there exists a universal electron trap density of $\approx 1\text{--}3 \times 10^{17} \text{ cm}^{-3}$, centered at an energy of $\approx 3.6 \text{ eV}$ below the vacuum level.^[14–17] This electron trap distribution is identical for a wide range of polymers considered. As possible origin, hydrated oxygen complexes were identified as cause for electron trapping.^[14–16] In addition, hole traps form continuously when operating PLEDs over many hours.^[18–20] Hole trap growth dictates the long-term stability of PLEDs.^[21]

Recently, we examined the dynamics of electron traps in PLEDs.^[22] We fabricated devices using a phenyl-substituted poly(*para*-phenylenvinylene) copolymer termed super yellow (SY) as emitting material (Figure S1, Supporting Information)^[23–28] and studied the device response to electrical driving and breaks. In an operated PLED traps are filled and after turning-off, deep electron traps de-trap slowly via thermal emission over many minutes. After every break, we observed an intermediate increase in device performance, and the initial light emission was higher and a lower voltage was required to drive a constant current. Subsequently, the voltage and light emission recovered back to the trend line before the break. This is because electron traps fill up again. Surprisingly, we found that filling of these traps is very slow and device recovery trends proceed over many minutes. This is in contrast to the general notion that trap filling is complete after a few hundreds of microseconds. Such a remarkable appearance is consistent with a slow diffusion process between precursor trap species that form a trap only when meeting, with the hydrated oxygen complex as a possible candidate.^[22] Because the electron trap density is constant, the light emission and voltage response to a break does not change over time, i.e., the same rest period at different moments leads to similar initial performance improvement and recovery trends.

Here, we first identify the same electron trap filling and de-trapping mechanism in SY PLECs. The analysis is more complicated than for a PLED, because relaxation and reconstruction of the EDLs occur on a similar time scale as electron trap filling and de-trapping. Therefore, electrical and optical transients in PLECs have to be analyzed as a superposition of effects due to a temporary imbalance in charge injection and electron trap filling. With the known electron trap density from PLEDs,^[15,22] we can quantify the experimental optical transients of the PLEC very well. Based on the identified similarity between PLEDs and PLECs, we then argue that during long-term operation also hole traps form in a PLEC. By virtue of the place where hole traps form in the active layer, we can conceptually distinguish between two types of hole traps, i.e., hole trap formation in the *i*-region and hole trap formation at the border between the *i*-region and the *p*-doped zone. The former hole traps primarily result in a decrease of the luminance. As for the electron traps, we can simulate the long-term luminance decay of the PLEC well by adopting the known hole trap formation rate from the PLED.^[21] The latter hole traps are specific to the PLEC device architecture and can be explained with the specific hole trap formation mechanism, which is based on the interaction between excitons with holes (*p*-polarons).^[21] In a PLEC, there is no physical separation between the position of exciton generation and

the doped zones. Therefore, part of the excitons is quenched due to the interaction with the high density of *n*- and *p*-polarons present in the doped zones. Exciton quenching via interaction with *p*-polarons results in hole trap formation. The outcome is that the *p*-doped region erodes over time and it needs a higher voltage to drive a constant current.

2. Results

2.1. Device Dynamics at Switch-On and After Switching Off

For SY PLECs with the added electrolyte trimethylolpropane ethoxylate/ $\text{Li}^+\text{CF}_3\text{SO}_3^-$, we discussed recently how the ionic rearrangement during device turn-on influences the light emission trend over many hours.^[11,29] At early times, the emitter position (EP) is close to the Al electrode and moves during operation over >30% of the active layer thickness toward the center. For an active layer thickness of below 150 nm, this EP shift results in a steady increase of the emitted light, while for thicknesses above 200 nm a valley of poor outcoupling efficiency is crossed. Directly after switch-on, the voltage decreases quickly due to the formation of EDLs and doped regions at both electrodes. Afterward, the voltage stays almost constant for a thin device and increases slowly for thicker active layers.^[11,29]

The added salt constituents play an important role on the transient device response when a PLEC is switched to short circuit and then back on to drive. First, we find that the *p*- and *n*-doping is very persistent and the necessary hold time at short circuit to equilibrate an operated thick PLEC is on the order of several days (Figure S2, Supporting Information). The time scale of days implies that a break of seconds to minutes does not affect the *p*- and *n*-doped regions.

Steady-state simulations in **Figure 1** under bias and directly after switching to short circuit indicate why doping relaxation is slow. Due to the increased conductivity of the doped zones, the electric field in these regions is small. The counter ions screen the field of the polarons, and although there is a large number of polarons, the net charge density is low. The built-in voltage at 0 V drops across the intrinsic region rather than across the doped regions (Figure 1). Although there is a large negative field in the intrinsic region, there are no ions present in this region that could relax.

On the other hand, the EDLs are regions with high electric fields and large ion density gradients. The former lead to high ion drift currents, the later to strong ion diffusion currents. These currents are in opposite directions and cancel each other in steady state at 3.6 V. When switching to 0 V, the ionic charge density does not change instantaneously, which means the diffusion current remains the same. However, the potential drop is reversed due to the built-in field, which reduces the field in the EDLs. This leads to a net ion current as indicated in Figure 1a.

We simulated the EDL relaxation over time by integrating the first 2 nm of the ion density at both electrodes after switching to 0 V (Figure 1c). In order to explain the measured color change of a thick PLEC over time, we reasoned previously that the mobility of the anions must be lower than the

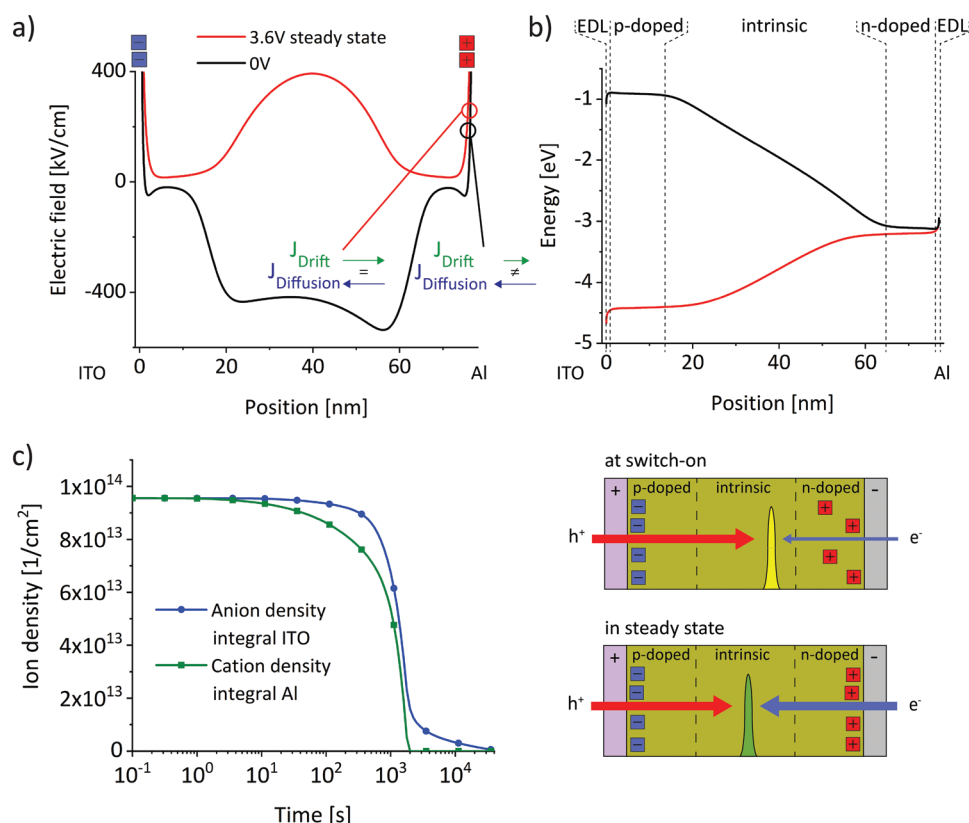


Figure 1. Drift-diffusion simulations on PLECs. a) Electric field and b) bending of the lowest unoccupied molecular orbital in steady state for a biased device (red) and immediately after 0 V is applied (black). The dynamic evolution of the electric double layers is shown in (c) by integrating the first 2 nm near the electrodes at different points in time after switching to short circuit. Since the cations are more mobile than the anions,^[11] the relaxation at the Al electrode is faster. The schematic in (c) illustrates that directly after switch-on following a break the emitter position is situated closer to the cathode and shifts toward the anode when the electric double layers recover. Simulation parameters are listed in Note S1 (Supporting Information).

cation mobility.^[11] Therefore, the cations at the Al electrode relax faster than the anions at the ITO electrode. This has the consequence that at switch-on the injection of electrons at the cathode is hindered, and lower than the injection of holes at the anode. This results in a temporary shift of the EP toward the Al electrode, as indicated in the schematic of Figure 1c. When the EDLs recover, charge injection balances and the EP moves back in direction of the ITO electrode to the position where it was before the break.

A small shift of the EP can result in a large change of the outcoupling efficiency, i.e., that part of emitted photons that actually leave the device.^[30,31] In Figure 2a, the luminance as a function of the EP is simulated for a 77 nm thick device. Due to interference of the direct emission with the reflected electromagnetic wave at the Al electrode, the luminance increases strongly when the EP shifts from the cathode to the anode with a peak luminance at around EP = 0.25.^[32] The simulation in Figure 2b shows that an even more informative, undulating luminance pattern with changing emission colors occurs for the 467 nm thick device. For the simulations we used the active layer thicknesses (77 or 467 nm) extracted from capacitance measurements, at low frequency and at $t = 0$.

By fitting measured EL spectra to an optical model, it is possible to track the position of the EP.^[11,30] We note that for thin devices the angle-dependent emission spectra are very similar

for different EPs. Thus, the EP cannot be determined reliably.^[33] Figure 2c shows experimental EL spectra from a thick device taken after driving for 7 and 8 h. After a break of 40 s, a first EL spectrum was measured immediately at switch-on, and a second spectrum when steady state was reached. The first spectrum after 8 h driving perfectly overlaps with the steady-state spectrum after 7 h. This means that during relaxation at 8 h the EP moved back to where it was in steady state after 7 h. We found before that 1 h of driving results in an EP shift of $\approx 1\%$ of the active layer thickness,^[11] which translates into an emission intensity change of 15–20% (Figure 2b). Figure S3 (Supporting Information), summarizes additional EL spectra for different driving times after relaxation and recovery. Data consistently confirm that the EP shifts from the Al electrode toward ITO after a break at 0 V.

2.2. Electron Trap Formation and Decay

Figure 3a,b shows long-term voltage and light emission trends for thick and thin PLECs, respectively. The current bias was paused after every hour and the device switched to short circuit for 40 s. The voltage overshoots after every switch-on and recovers back to the trend line. We ascribe this to the relaxation of the EDLs during rest at short circuit, which deteriorates the

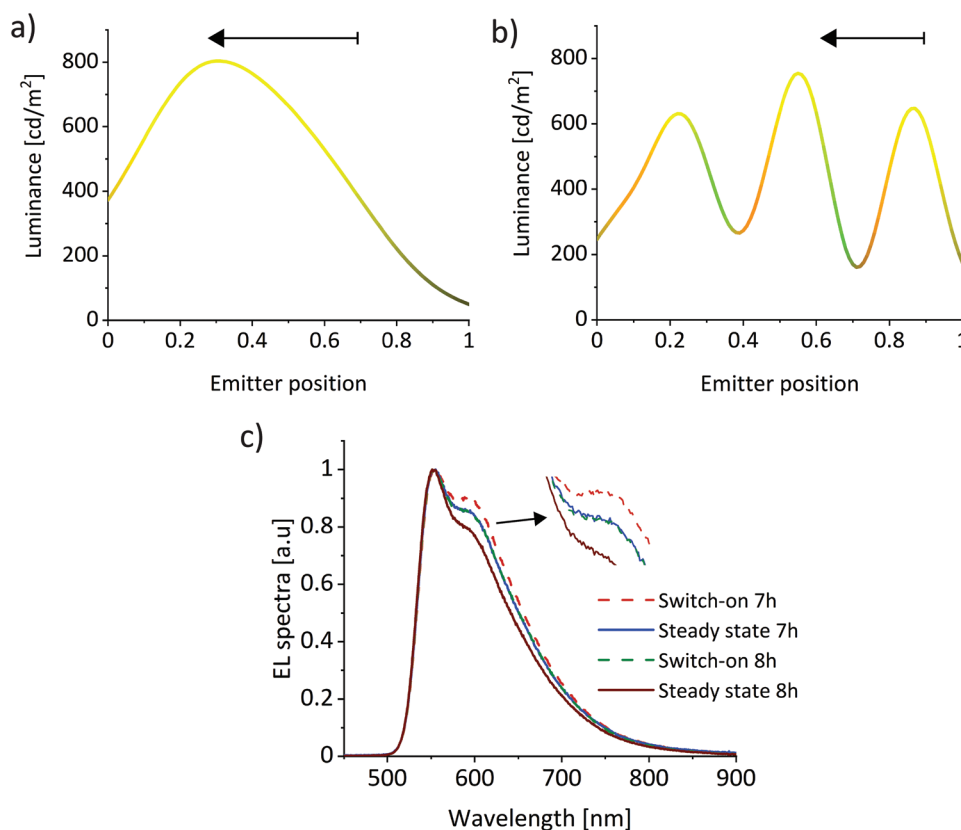


Figure 2. Optical simulations on PLECs. Luminance versus emitter position for a) a 77 nm thick SY layer and b) a 467 nm thick SY layer. In both cases, a constant current of 7.7 mA cm^{-2} was assumed. Emitter position = 1 indicates the Al electrode, emitter position = 0 is the ITO electrode. The line color represents the emitted color at the given emitter position. Experimental long-term emitter position shifts during operation are indicated by arrows. c) Normalized electroluminescence (EL) spectra of a 450 nm thick PLEC after an operation time of 7 and 8 h. Spectra were measured directly after switch-on following a relaxation time of 40 s at 0 V, and 50–70 s later (close to steady state). Spectra at switch-on were more intense than the respective steady-state spectra by +12% at 7 h, and by +16% at 8 h. The actual color of the emitted light after 7 and 8 h of operation was red.

initial charge injection and a higher voltage is required to drive a constant current until the EDLs have established again.

Also, the light emission from the thick device (Figure 3a) overshoots at switch-on, but the magnitude is not constant over time, despite a steady break time. The light emission from the thin device (Figure 3b) starts first at lower values and changes to positive emission spikes shortly before steady state, where the emitted light reaches a plateau.

Figure 3a,b includes magnifications of the transients after an operation time of 7 h. While for the thick device the light decay appears monotonic, the transient for the thin device shows an oscillatory behavior, it starts below the trend line but then overshoots before approaching steady state. We interpret that this behavior is the result of superimposing effects due to EDL reconstruction and electron trap filling. Both effects influence the luminance at switch-on differently and have a slightly different time constant, which we disentangle in the following.

EDLs relax during the break at 0 V and this results in a shift of the initial EP at switch-on, as explained above. We kept the break time constant at 40 s over the whole measurement time and assume that also the EP shift is constant. However, a constant EP shift results in different emission spikes, depending on the actual EP (Figure 2). We illustrate this effect for the

thick device at different points in time in Figure 3c. The simulated luminance trend assumes an EP shift with a constant speed of 0.01 h^{-1} from 0.9 to 0.6 over an operation time of 30 h (Figure 2b). For the relaxation during each break, we adopt the value of 0.01 EP, as discussed for the device situation after an operation time of 8 h (Figure 2c).

The simulated light emission trend in Figure 3c does not agree with the measurement, especially since the simulated emission spike is negative for EPs between 0.68 and 0.6. To replicate the experiment, we need to add a constant positive light overshoot of $\approx 15\%$ of a particular light level to the emission after every break (Figure 3d). This overshoot is the result of electron de-trapping at rest.^[22] At switch-on, the light temporarily increases because non-radiative SRH recombination between trapped electrons and free holes is small. Trap filling during operation increases SRH recombination and the light recovers to the trend line before the break. We illustrate the light emission trend due to electron de-trapping at rest—followed by trap filling during operation—separately with a PLED, because a PLED contains no salt and EDL relaxation is not present (Figure S4, Supporting Information).

The combination of EDL relaxation and electron de-trapping at rest also explains the light emission trend of the thin device

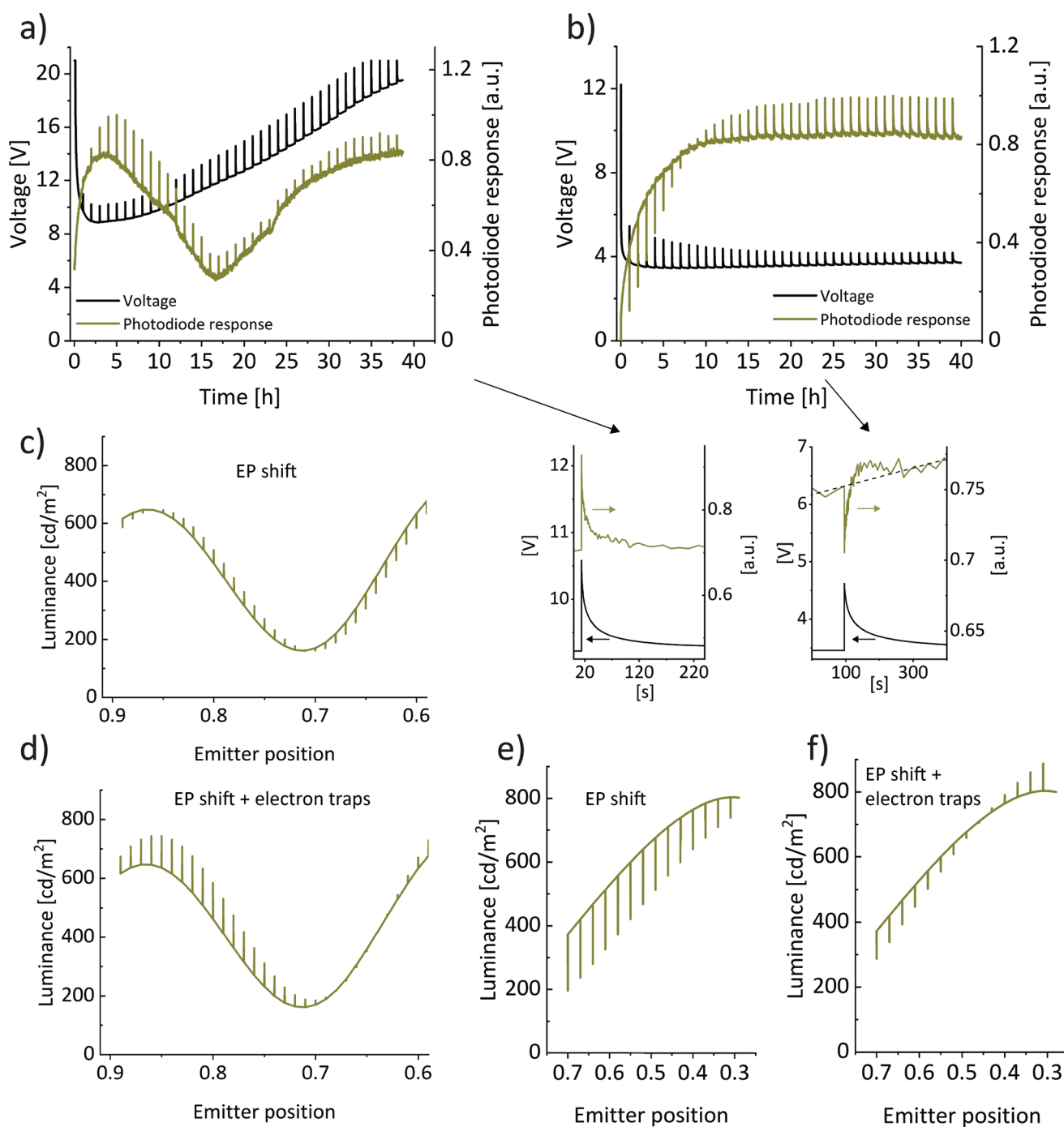


Figure 3. Long-term performance of PLECs. Voltage and light emission trends over 40 h for constant current-driven (7.7 mA cm^{-2}) PLECs with an active layer thickness of a) 450 nm and b) 75 nm. After every hour, the device was rested for 40 s at short circuit. Included are magnifications of a) and b) after 7 h driving. c–f) Simulated light emission characteristics for thick (c,d) and thin (e,f) PLECs.

(Figure 3b). The effect of EDL relaxation alone results in a permanent light undershoot at turn-on (Figure 3e). When adding a constant positive emission spike, the experimental change of sign after 7 h is reproduced (Figure 3f). We simulated the luminance as function of the electron trap site density and found that the observed light overshoot of $\approx 15\%$ at switch-on corresponds to an electron trap site density of $\approx 0.5 \times 10^{17} \text{ cm}^{-3}$

that decayed during the relaxation time of 40 s (Note S2, Supporting Information). This is in good agreement with observations made for PLEDs.^[22] Finally, both PLECs show after rest a positive voltage overshoot throughout. This indicates that the voltage undershoots due to charge de-trapping^[22] is masked by a stronger voltage increase due to EDL relaxation (Figure S4, Supporting Information).

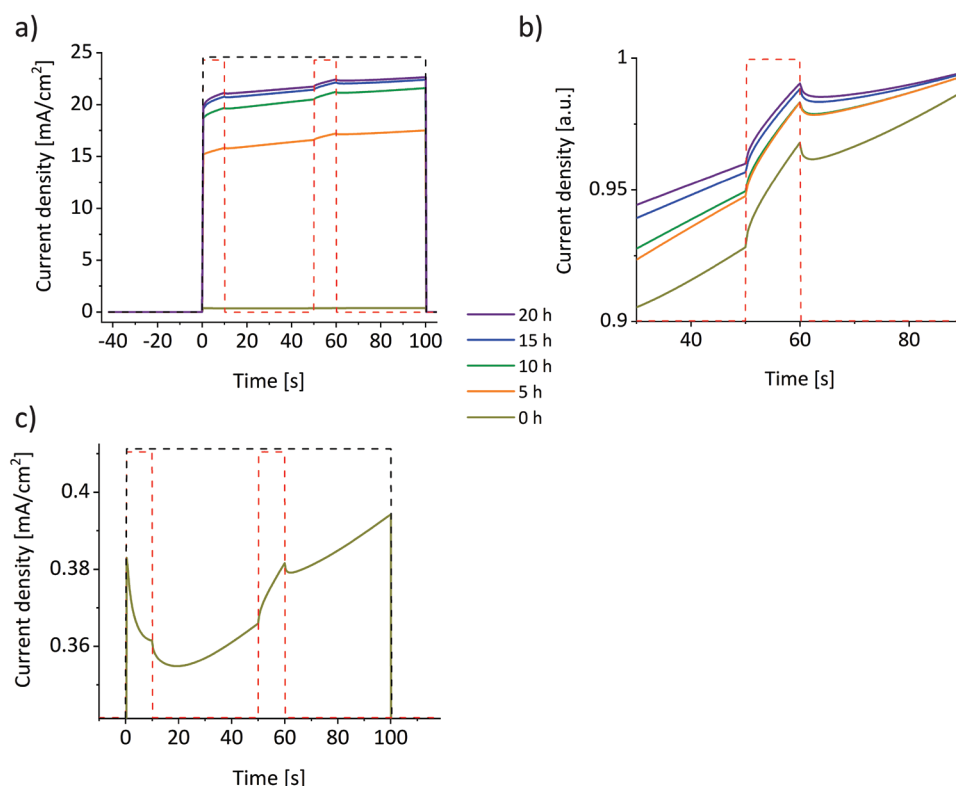


Figure 4. a) A 75 nm thick PLEC was biased at a constant current of 7.7 mA cm^{-2} . After every hour a break (40 s) at short circuit was applied, followed by a voltage pulse of 6 V for 100 s (black, dashed line). The current level increases from $\approx 0.4 \text{ mA cm}^{-2}$ at 0 h, to above 20 mA cm^{-2} after 20 h driving; this increase is due to the formation of the EDLs and doped zones. Directly at switch-on and after 50 s, the device was irradiated (photon flux $1.4 \times 10^{21} \text{ s}^{-1} \text{ m}^{-2}$) for 10 s with light at 656 nm (red, dashed line). b) Normalized current trends from a) to illustrate the constant influence of light on the current during the second irradiation. c) Current trend for a pristine device with light pulses applied.

2.3. Electron De-Trapping by Light

We obtain further evidence for electron traps in the PLEC from illumination experiments with light at 656 nm, which is below the bandgap of SY.^[34] Data in **Figure 4** show that the current increases during the light pulse and recovers afterward to the trend line. This trend indicates that light irradiation induces electron de-trapping, which results in a decrease of immobile trapped charge and an increase of the current.^[22] The current dynamics during the light pulse and the recovery trend after switching off the light (i.e., formation of electron traps) for a PLEC and a PLED match, because the underlying mechanism is the same (Figure S8, Supporting Information).

The current increase during the light pulse and the relaxation is independent of the operation time (Figure 4b). This indicates that the process does not involve hole traps, because they form continuously and grow in number over time. At the same time, the trend also excludes an involvement of the *n*- and *p*-polarons that absorb light below the SY bandgap as well and slowly grow over many hours.^[29,34] The current increase occurs even for a pristine device during light irradiation already after 50 s, when doped zones are not yet present (Figure 4c). The current decrease of the pristine device during the first 20 s in Figure 4c is due to electron trap filling, as observed for PLEDs.^[22] Afterward, EDLs form and the overall current starts to increase.

2.4. Device Degradation During Long-Term Operation

To investigate the long-term device stability, we turn to absorption measurements during biasing. Therefore, a device was operated at a constant voltage over >20 h. After every hour, the voltage bias was stopped and the absorption at different voltages was measured. **Figure 5a** displays the electroabsorption (EA) signal at 514 nm. At this wavelength, we probe the absorption of SY (Figure S9, Supporting Information). The signal is due to the Stark effect and thus is a measure of the electric field in the device.^[35] Because the field is strongest in the *i*-region (Figure 1a) and the voltage drop is constant across this region after EDL formation, the Stark signal is a measure for the thickness of the *i*-region. The EA signal is proportional to the product of the optical density, i.e., the film thickness, and the square of the electric field. When the electric field concentrates in a shrinking *i*-region, the Stark effect intensity increases because the quadratic signal gain due to the higher electric field overcompensates the linear signal decrease due to the thinner region where the signal originates from. Specifically, the peak at 3 h in Figure 5a indicates that the electric field at this time is strongest, i.e., the *i*-region is the thinnest. The subsequent decrease of the signal indicates that the *i*-region expands over time. The EA signal approaches a plateau after ≈ 12 h, indicating the ion motion slows down. Capacitance measurements confirm that the *i*-region is the

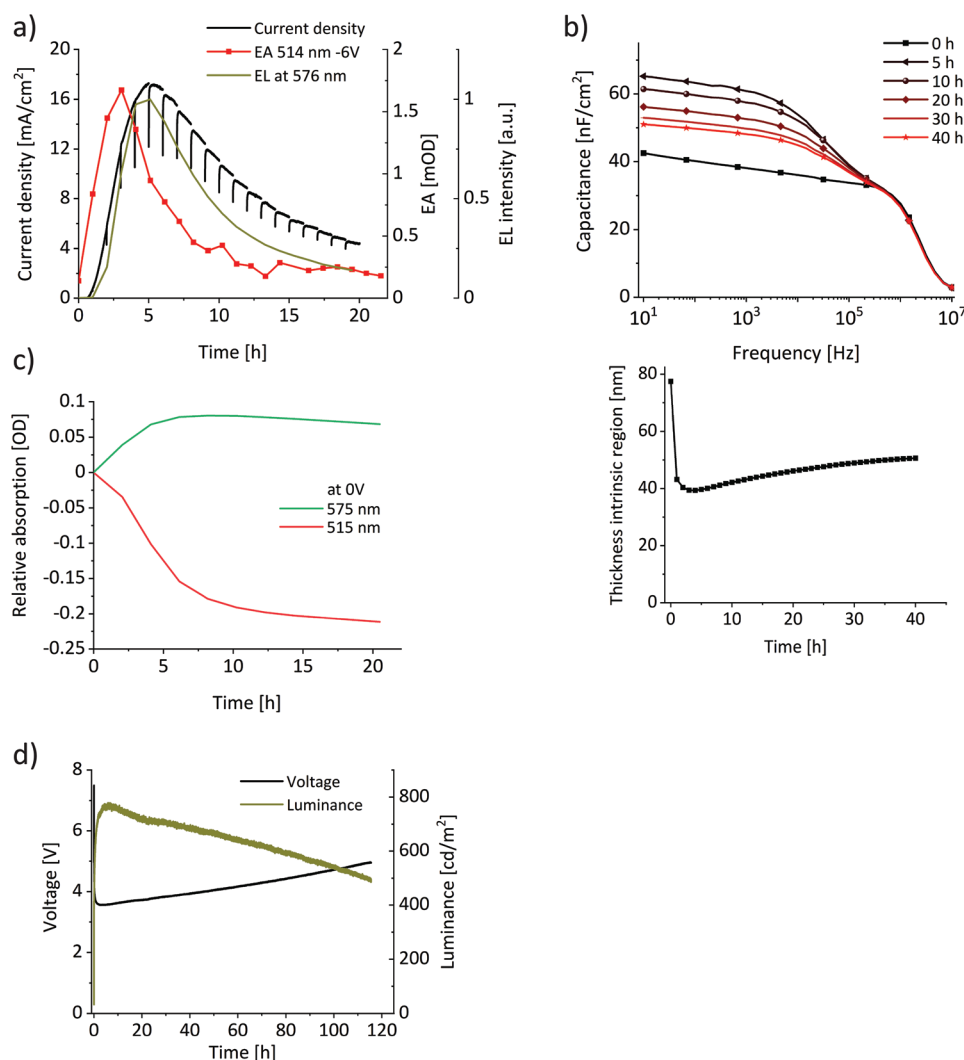


Figure 5. a) Current, light and absorption transients of a 450 nm thick constant voltage-driven PLEC (12 V). Shown is the absorption at 514 nm that was measured at -6 V, relative to the absorption at 0 V. b) Capacitance versus frequency dynamics of a 75 nm thick PLEC, measured on the pristine device and during constant-current operation (7.7 mA cm^{-2}). The thickness of the low-conductive region was calculated from the capacitance at 300 Hz. c) Change of absorption over time of a 75 nm thick PLEC relative to the absorption of the pristine device. The absorption of the pristine device was 0.74 OD at 515 nm, and 0.03 OD at 575 nm. d) Long-term voltage and luminance trends of a constant-current (7.7 mA cm^{-2}) driven 75 nm thick PLEC.

thinnest after an operation time of 3 h (Figure 5b; Figure S10, Supporting Information). Afterward, the width of the low conductivity part of the device increases very slowly out to a measurement time of 40 h.

Included in Figure 5a are the current density and EL signal. In contrast to the EA signal, the current and light transients decrease continuously during the measurement from 12 to 20 h, which is a signature of device degradation. Note that the light and current decay show the same trend; this confirms that the shift of the EP has stopped after ≈ 12 h.^[11]

Figure 5c displays changes of absorptions at two wavelengths over time. At 515 nm we follow the absorption change of SY. We chose the wavelength 575 nm to detect (mainly) changes of the *p*-polaron density, the absorption of the *n*-dopants at this wavelength is very small (Figure S9, Supporting Information).^[34] The increase of the absorption at 575 nm during the first ≈ 9 h is due to the growth of the doped zones. Radical cations and

anions form from the parent SY, which explains the absorption decrease at 515 nm.^[36] For longer times, the absorptions at both wavelengths slightly decrease with a similar trend. Again, we ascribe this observation to device degradation.

Figure 5d displays the long-term voltage and luminance trends over 115 h of a constant-current driven thin PLEC. Due to the dynamic turn-on behavior of the PLEC, the voltage continuously decreases during the first few hours and the luminance increases slowly. The maximum power efficacy is 8.7 lm W^{-1} after 5 h, and the efficacy drops during operation to 5.8 lm W^{-1} (after 70 h) and 4.2 lm W^{-1} (after 110 h). We compared the stability of the PLEC with a PLED during the operation time from 5 and 70 h (Figure S11, Supporting Information). The relative decrease of the luminance for the two device was almost the same (PLED -15% , PLEC -18%), but the relative voltage increase of the PLEC ($+20\%$) was clearly larger than for the PLED ($+5\%$). In the following discussion, we bring forward

the argument that the larger voltage increase for the PLEC is due to additional hole trap formation at the border between the *i*-region and the *p*-doped zone.

3. Discussion

We detect electron traps in PLECs by measuring the device response to electrical driving and breaks. This measurement sequence involves a change in temperature. During break, the power is zero and the device temperature relaxes to room temperature. At switch-on, the electrical power heats up the sample until steady state between heat loss and electrical heating is reached. A changing temperature influences, for example, the charge mobility values and the photoluminescence quantum efficiency. This change in temperature, however, does not influence our measurements. We observed that the temperature adjusts in <10 s, which is much faster than the observed recovery times after switch-on (Figure S12, Supporting Information; and >200 s in Figure 3).

We find that the electron trap site density and the dynamics of electron trap formation and decay in the PLEC and the PLED are identical (Note S2, and Figure S8, Supporting Information). This is indeed expected, because electron traps originate from the semiconducting polymer, which is the same for both devices.

We turn to the identification and approximate quantification of hole traps in the PLEC. Details of the following discussion are summarized in the Note S2 (Supporting Information). As a first approximation, we assumed that the experimental long-term performance decay (Figure 5) is solely due to hole trap formation. In the PLED, long-term device degradation is attributed to hole traps that continuously form via exciton-*p*-polaron interactions.^[21] The energy of the exciton is transferred to the hole, which is excited to higher energetic states. Subsequently, bonds breaking in some of these excited *p*-polarons can produce hole traps directly, or hole traps can form via further interactions with adjacent molecules.^[20] The efficacy (cd A⁻¹) of a SY PLED and PLEC are comparable;^[29,37] thus, the exciton densities are similar. Non-radiative SRH recombination between free electrons and trapped holes reduces the luminance. This mechanism is important in the *i*-region of the PLEC, where the density of free electrons is high. From numerical simulation, we can estimate how much the luminance decreases for a certain number of added hole traps. We adopted the known rate of hole trap formation for PLEDs^[21] and with this could simulate the experimental luminance trend of the PLEC shown in Figure 5d very well (Note S2, Supporting Information).

However, there are several pieces of evidence that suggest that an additional fraction of hole traps forms in the PLEC. These additional traps are not involved in SRH recombination and therefore do not form in the *i*-region. We propose that these hole traps form at the interface between the *i*-region and the *p*-doped zone. The stabilized polaron density (> 10¹⁸ cm⁻³) in the doped regions of a PLEC is much higher than the free polaron density (a few times 10¹⁷ cm⁻³) in the PLEC *i*-region and the PLED^[18,21,22] (Figure S7, Supporting Information). Therefore, we propose that additional hole traps form at the border between the *p*-doped and the *i*-region. When a hole trap forms, the positive mobile charge of the stabilized *p*-dopant is replaced

by the immobile positive charge of the hole trap. Thereby, the width of the *i*-region, or more precisely the width of the low conductive region, increases.

A first indication for additional hole traps in PLECs comes from the experimental voltage increase (+8.8% between 10 and 40 h, Figure 5d), which is much larger than the simulated PLEC voltage increase (+2%, Figure S6, Supporting Information) with the adopted hole trap density from PLEDs. As a qualitative argument, this means that when the low conductive region widens due to additional hole trap formation, it needs a higher voltage to drive a constant current.

Additional hole trap formation can also be estimated from the long-term absorption and capacitance measurements. From Figure 5c, it can be seen that the absorption at 575 nm decreases between 10 to 20 h by -15%. If we assume that the absorption at 575 nm is solely due to *p*-polarons, then this decrease indicates that 15% of the *p*-polarons were consumed because of hole trap formation. From Figure 5b, it can further be seen that the low conductive region widens by 4 nm during this time. From the simulated capacitance, we determined the border of the *p*-doped region at 10 h (that was at 15 nm), and estimated from the simulated charge density profiles where this border shifts when 15% of the *p*-polaron density is removed (to 10 nm, Figure S7, Supporting Information). The simulated increase of the *i*-region (5 nm) agrees well with the experimental increase (4 nm) of the low-conductive region obtained from capacitance measurements.

To summarize, we can conceptually distinguish between two types of hole traps in a PLEC. A fraction of hole traps forms during operation in the *i*-region. These hole traps increase the SRH recombination between free electrons and trapped holes and are responsible for the observed luminance decrease over time. The hole trap formation rate in the intrinsic zone of a PLEC and in a PLED is quite comparable. In addition, hole traps form in a PLEC at the border between the *i*- and the *p*-doped region. The influence of these hole traps on the luminance (decrease) is small, because the density of free electrons at this border is small. The negative influence of these hole traps becomes mainly apparent via the measured voltage increase during operation, which was much larger for the PLEC than for a PLED. Interestingly, the long-term decay of the SY and *p*-polaron absorption show a similar trend (Figure 5c). This suggests a hole trap formation mechanism that consumes *p*-dopants and parent SY polymer repeating units at the same time.

Clearly, our hole trap formation analysis involves a number of assumptions. For example, the assumption that the light absorption at 575 nm is solely due to *p*-polarons is not entirely true, because also *n*-polarons absorb at this wavelength slightly.^[34] It is also not assured that every *p*-polaron that decays is transformed into a hole trap. Therefore, our analysis does not imply that no other long-term degradation mechanisms are operative in a PLEC. Results suggest, however, that hole trap formation in PLECs constitutes an important long-term degradation mechanism, as firmly established for PLEDs.

4. Conclusions

We have demonstrated the presence of electron traps and the formation of hole traps during operation in SY PLECs. The

electron trap density and the dynamics of electron trap formation and decay in a PLEC is the same as in a PLED. Likewise, the hole trap formation rate in a PLED and in the *i*-region of a PLEC match. When using the same active light-emitting polymer, this is indeed expected. However, we found that in the PLEC a considerable fraction of additional hole traps forms at the border between the *i*-region and the *p*-doped zone. Charge traps reduce the PLEC performance and influence the long-term stability to a large extent. So far, experiments to increase the operational stability of PLECs were mostly targeted on optimizing the electrolyte concentration, stabilizing the *p*-*i*-*n* configuration, applying pulsed versus continuous driving schemes, or preventing electrochemical side reactions of the electrolyte.^[2,5,38–41] Such attempts involved the variation of polymer-extrinsic parameters that can be varied, if necessary. Charge traps represent more fundamental performance-limiting sources, as they concern the light-emitting polymer directly.

5. Experimental Section

PLECs were fabricated in the configuration glass/ITO(Geomatec, 11 Ω square^{−1})/SY + Li⁺CF₃SO₃[−] + TMPE, (75 ± 10 nm) or (450 ± 40 nm)/Al(70 nm), PLEDs in the configuration glass/ITO/PEDOT:PSS(HTL Solar, 40 nm)/SY(80 ± 10 nm)/Ca(10 nm)/Al(70 nm). Layer thicknesses were measured with an Ambios XP1 profilometer. PEDOT:PSS films were spin coated from filtered (pore size 0.45 μm) solution and were then dried for 20 min at 120 °C. Dried (24 h, 0.1 mbar, 40 °C) SY (Merck) and dried (24 h, 0.1 mbar, 160 °C) Li⁺CF₃SO₃[−] (Sigma–Aldrich) together with dried (24 h, 0.1 mbar, room temperature) TMPE (trimethylolpropane ethoxylate, Sigma–Aldrich, average *M_n* 450) were separately dissolved in anhydrous tetrahydrofuran (THF, Sigma–Aldrich). The concentrations for salt and TMPE were 10 mg mL^{−1}, for SY 5 mg mL^{−1} (thin PLEC and PLED) or 12 mg mL^{−1} (thick PLEC). Precursor solutions were stirred for 7 h at 60 °C inside a glove box (H₂O < 1 ppm, O₂ < 20 ppm). For PLECs, the precursor solutions were mixed in mass ratios of 1:0.1:0.03 (SY:TMPE:Li⁺CF₃SO₃[−]) and were then stirred for at least 17 h at 60 °C.^[29] Before spin coating, solutions were let to cool down for 20 min. Non-filtered solutions were used for film coating. Calcium and aluminum were thermally evaporated through a shadow mask defining eight cells with an active area of 3.1 or 7.1 mm² per substrate. Details on the PLED and PLEC fabrication are summarized in references.^[11,22]

Electroluminescence spectra were measured with an integrating sphere on an Ocean Optics spectrometer QE Pro, calibrated before each measurement. Angular dependent EL measurements were performed with the Phelos measurement system (Fluxim AG, Switzerland). Impedance measurements at 0 V with an alternating 70 mV signal to determine the capacitance transients were performed on the Paios measurement system (Fluxim AG, Switzerland), as well as the current and light intensity transients. The light intensity was measured with a photodiode as photovoltage. The relation between the measured photovoltage and the corresponding radiance/luminance is explained in the Supporting Information of reference.^[11]

Optical and electrical simulations were performed with Setfos 5.1 (Fluxim AG, Switzerland). Simulation procedures and parameters are described in the Supporting Information. The refractive indices for the intrinsic SY layer were confirmed by simulation of experimental transmission spectra measured previously.^[29]

EA data were collected in a reflection configuration, where *p*-polarized light hits the device at an angle of 45 degrees through the transparent electrode side and was reflected outward by the metallic electrode, thus making two passes through the SY layer. A Cree XP-E white-light LED powered by a Mastech 3010D DC supply was used as light source. Light propagation from the LED to the sample and further to the spectrometer Andor Shamrock 500i equipped with an Andor Newton

DU970 CCD camera was aligned in a simple optical scheme with lenses. EA scans were performed during interruptions of the constant voltage operation. For each scan, a ramp pulse of 150 ms was applied to the sample by a Tektronix AFG 3101 function generator (the same as used for DC biasing) with the amplitude starting at 12 V (DC operation bias), reaching −6 V and again increasing to 12 V. The detecting camera, capturing 200 spectra per ramp period, was synchronized to the ramp sequence. Data were averaged from 375 pulses. Thus, individual spectra in the dataset correspond to a certain voltage applied to the sample. The light intensity at 0 V was taken as reference and the EA, i.e., the change of the light intensity versus voltage, was calculated in OD units. Variation of the absolute intensity of the detected light with operation time enabled to estimate long term changes of the sample absorption. The same spectrometer and camera were used to record EL spectra during operation while blocking the light from the LED with a computer-controlled shutter.

Supporting Information

Supporting Information is available from the Wiley Online Library or from the author.

Acknowledgements

Financial support from the Swiss National Science Foundation (grant IZBRZ2_186261 and P500PT_203221) was acknowledged.

Open access funding provided by ETH-Bereich Forschungsanstalten.

Conflict of Interest

The authors declare no conflict of interest.

Data Availability Statement

The data that support the findings of this study are available in the supplementary material of this article.

Keywords

degradation, electron traps, hole traps, lifetime, polymer light emitting diodes, polymer light emitting electrochemical cells

Received: March 31, 2022

Revised: August 5, 2022

Published online: August 21, 2022

- [1] J. Ràfols-Ribé, X. Zhang, C. Larsen, P. Lundberg, E. M. Lindh, C. T. Mai, J. Mindemark, E. Gracia-Espino, L. Edman, *Adv. Mater.* **2022**, 34, 2107849.
- [2] S. Tang, L. Edman, *Top. Curr. Chem (Z)* **2016**, 374, 40.
- [3] S. B. Meier, D. Tordera, A. Pertegás, C. Roldán-Carmona, E. Ortí, H. J. Bolink, *Mater. Today* **2014**, 17, 217.
- [4] J. Mindemark, S. Tang, H. Li, L. Edman, *Adv. Funct. Mater.* **2018**, 28, 1801295.
- [5] J. Gao, *Chem. Plus. Chem.* **2018**, 83, 183.
- [6] K. Youssef, Y. Li, S. O'Keeffe, L. Li, Q. Pei, *Adv. Funct. Mater.* **2020**, 30, 1909102.

- [7] J. Ràfols-Ribé, N. D. Robinson, C. Larsen, S. Tang, M. Top, A. Sandström, L. Edman, *Adv. Funct. Mater.* **2020**, *30*, 1908649.
- [8] E. Fresta, R. D. Costa, *Adv. Funct. Mater.* **2020**, *30*, 1908176.
- [9] L. Mardegan, C. Dreessen, M. Sessolo, D. Tordera, H. J. Bolink, *Adv. Funct. Mater.* **2021**, *31*, 2104249.
- [10] S. van Reenen, R. A. J. Janssen, M. Kemerink, *Adv. Funct. Mater.* **2012**, *22*, 4547.
- [11] M. Diethelm, A. Schiller, M. Kawecki, A. Devižis, B. Blülle, S. Jenatsch, E. Knapp, Q. Grossmann, B. Ruhstaller, F. Nüesch, R. Hany, *Adv. Funct. Mater.* **2020**, *30*, 1906803.
- [12] S. Tang, J. Mindemark, C. M. G. Araujo, D. Brandell, L. Edman, *Chem. Mater.* **2014**, *26*, 5083.
- [13] N. B. Kotadiya, A. Mondal, P. W. M. Blom, D. Andrienko, G.-J. A. H. Wetzelaer, *Nat. Mater.* **2019**, *18*, 1182.
- [14] M. Kuik, G.-J. A. H. Wetzelaer, H. T. Nicolai, N. I. Craciun, D. M. De Leeuw, P. W. M. Blom, *Adv. Mater.* **2014**, *26*, 512.
- [15] H. T. Nicolai, M. Kuik, G. A. H. Wetzelaer, B. de Boer, C. Campbell, C. Risko, J. L. Brédas, P. W. M. Blom, *Nat. Mater.* **2012**, *11*, 882.
- [16] D. Abbaszadeh, A. Kunz, N. B. Kotadiya, A. Mondal, D. Andrienko, J. J. Michels, G.-J. A. H. Wetzelaer, P. W. M. Blom, *Chem. Mater.* **2019**, *31*, 6380.
- [17] D. Abbaszadeh, A. Kunz, G. A. H. Wetzelaer, J. J. Michels, N. I. Craciun, K. Koyunov, I. Lieberwirth, P. W. M. Blom, *Nat. Mater.* **2016**, *15*, 628.
- [18] Q. Niu, G.-J. A. H. Wetzelaer, P. W. M. Blom, N. I. Craciun, *Adv. Electron. Mater.* **2016**, *2*, 1600103.
- [19] Q. Niu, G.-J. A. H. Wetzelaer, P. W. M. Blom, N. I. Craciun, *Appl. Phys. Lett.* **2019**, *114*, 163301.
- [20] I. Rörich, Q. Niu, B. van der Zee, E. d. P. Rosendo, N. I. Craciun, C. Ramanan, P. W. M. Blom, *Adv. Electron. Mater.* **2020**, *6*, 1700643.
- [21] Q. Niu, R. Rohloff, G.-J. A. H. Wetzelaer, P. W. M. Blom, N. I. Craciun, *Nat. Mater.* **2018**, *17*, 557.
- [22] M. Diethelm, M. Bauer, W.-H. Hu, C. Vael, S. Jenatsch, P. W. M. Blom, F. Nüesch, R. Hany, *Adv. Funct. Mater.* **2022**, *32*, 2106185.
- [23] S. Burns, J. MacLeod, T. T. Do, P. Sonar, S. D. Yambem, *Sci. Rep.* **2017**, *7*, 40805.
- [24] S. Tang, L. Edman, *J. Phys. Chem. Lett.* **2010**, *1*, 2727.
- [25] M. Kawecki, R. Hany, M. Diethelm, S. Jenatsch, Q. Grossmann, L. Bernard, H. J. Hug, *ACS Appl. Mater. Interfaces* **2018**, *10*, 39100.
- [26] B. Van der Zee, Y. Li, G.-J. A. H. Wetzelaer, P. W. M. Blom, *Adv. Mater.* **2022**, *34*, 2108887.
- [27] Y. Noguchi, T. Higeta, F. Yonekawa, *Adv. Optical Mater.* **2018**, *6*, 1800318.
- [28] H. Iwakiri, H. Watanabe, Y. Noguchi, *ACS Appl. Electron. Mater.* **2021**, *3*, 2355.
- [29] M. Diethelm, Q. Grossmann, A. Schiller, E. Knapp, S. Jenatsch, M. Kawecki, F. Nüesch, R. Hany, *Adv. Opt. Mater.* **2019**, *7*, 1801278.
- [30] S. Jenatsch, M. Regnat, R. Hany, M. Diethelm, F. Nüesch, B. Ruhstaller, *ACS Photonics* **2018**, *5*, 1591.
- [31] E. M. Lindh, P. Lundberg, T. Lanz, L. Edman, *Sci. Rep.* **2019**, *9*, 10433.
- [32] H. Becker, S. E. Burns, R. H. Friend, *Phys. Rev. B* **1997**, *56*, 1893.
- [33] M. Flämmich, D. Michaelis, N. Danz, *Org. Electronics* **2011**, *12*, 83.
- [34] T. Lanz, E. M. Lindh, L. Edman, *J. Mater. Chem. C* **2017**, *5*, 4706.
- [35] A. Devižis, A. Gelzinis, J. Chmeliov, M. Diethelm, L. Endriukaitis, D. Padula, R. Hany, *Adv. Funct. Mater.* **2021**, *31*, 2102000.
- [36] S. Jenatsch, L. Wang, M. Bulloni, A. C. Véron, B. Ruhstaller, S. Altazin, F. Nüesch, R. Hany, *ACS Appl. Mater. Interfaces* **2016**, *8*, 6554.
- [37] J. Ràfols-Ribé, E. Gracia-Espino, S. Jenatsch, P. Lundberg, A. Sandström, S. Tang, C. Larsen, L. Edman, *Adv. Optical Mater.* **2021**, *9*, 2001405.
- [38] J. Fang, P. Matyba, L. Edman, *Adv. Funct. Mater.* **2009**, *19*, 2671.
- [39] J. Gao, G. Yu, A. J. Heeger, *Appl. Phys. Lett.* **1997**, *71*, 1293.
- [40] J. M. Leger, D. B. Rodovsky, G. P. Bartholomew, *Adv. Mater.* **2006**, *18*, 3130.
- [41] D. Tordera, S. Meier, M. Lenes, R. D. Costa, E. Ortí, W. Sarfert, H. J. Bolink, *Adv. Mater.* **2012**, *24*, 897.